Optics Letters

Regenerative Fourier transformation for dual-quadrature regeneration of multilevel rectangular QAM

Mariia Sorokina,* Stylianos Sygletos, Andrew Ellis, and Sergei Turitsyn

Aston Institute of Photonic Technologies, Aston University, B4 7ET Birmingham, UK
**Corresponding author: m.sorokina@aston.ac.uk*

Received 20 April 2015; revised 11 June 2015; accepted 11 June 2015; posted 11 June 2015 (Doc. ID 238413); published 26 June 2015

We propose a new nonlinear optical loop mirror based configuration capable of regenerating regular rectangular quadrature amplitude modulated (QAM) signals. The scheme achieves suppression of noise distortion on both signal quadratures through the realization of two orthogonal regenerative Fourier transformations. Numerical simulations show the performance of the scheme for high constellation complexities (including 256-QAM formats).

OCIS codes: (060.2330) Fiber optics communications; (230.1150) All-optical devices; (230.4320) Nonlinear optical devices.

http://dx.doi.org/10.1364/OL.40.003117

The increasing capacity demand in optical networks has required the use of complex quadrature amplitude modulated (QAM) formats characterized by multilevel encoding in amplitude and phase. Despite its spectral efficiency benefits, the QAM modulation is highly sensitive to fiber link distortions [1] and thus unable to support transmission over ultra-long haul distances. All-optical regeneration, by enabling the periodic restoration of the signal quality along the link, has the potential to address this issue and to match the diverse requirements of high capacity and long haul networking.

Despite the recent developments in the design and implementation of new all-optical regeneration techniques, there is still a lack of a generic approach to deal with QAM constellations of any order offering simultaneous suppression of amplitude and phase noise. The phase quantizer, proposed in [2], is limited to phase shift keyed (M-PSK) encoded waveforms and it does not suppress the amplitude distortion. Combining the scheme with a phase preserving nonlinear optical loop mirror (NOLM) [3] amplitude noise suppression also could be provided [4]; however, dual-quadrature regeneration for more than two amplitude levels has not been shown yet [5]. A more advanced NOLM scheme has been proposed in [6] to deal with an increased number of amplitude levels, but it is still limited to circular QAM signals. As rectangular QAMs are becoming the prevailing format in optical communications, suitable regenerator solutions will be required accordingly.

Toward this direction, removal of the distortion from both signal quadratures has been shown in [7] by combining self-phase modulation induced phase shifting and PSA-based quadrature squeezing to regenerate each amplitude level. The scheme is highly efficient, but its complexity scales proportionally to the number of amplitude levels at each signal quadrature. Recently in [8], we introduced the regenerative Fourier transformation (RFT) and showed that the first-order Fourier expansion of an ideal step-wise regenerator enables an infinite number of regenerative levels on each signal quadrature. When applied in transmission lines, the RFT can provide Shannon capacities beyond the linear Shannon limits [8] and, as such, its all-optical realizations are highly desirable for future networks.

In this Letter, we propose a new all-optical design of the RFT, based on the use of a novel NOLM configuration. Contrary to the traditional phase insensitive schemes [4,6,9], here the nonlinear phase shift is achieved through coherent mixing of the signal with a local pump. This creates a sinusoidal transformation on the amplitude and not on the power of the input field. Furthermore, unlike [10,11], the interferometer operates in an asymmetric mode, i.e., the pump interacts only with the counter-propagating wave, allowing for the required beating of the original signal with its nonlinear transformed to realize the RFT. This unique combination of properties makes the proposed scheme compatible with conventional rectangular QAM signals of any duty cycle and constellation order with performance close to that of an ideal regenerator.

The RFT transfer function is the first-order expansion in the Fourier series of the step-wise transfer function (TF); therefore, it represents a smooth and close approximation of an ideal regenerator. Indeed, a step-wise TF with step $2x_0$ is given by

$$y_{\text{ideal}} = x - \text{mod}(x, 2x_0) + x_0. \quad (1)$$

By expanding the mod operator in Fourier series, we get

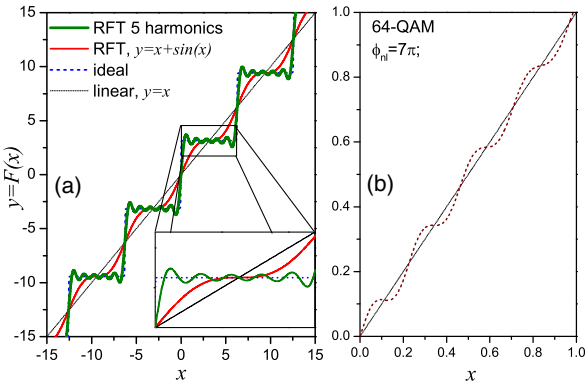

Fig. 1. Transfer functions of RFT compared with step-wise response of an ideal regenerator (a) as given by Eq. (2) for different number of harmonics and (b) its optical realization by the scheme of Fig. 2 for regenerating 64-QAM signals.

$$y_{\text{ideal}} = x - \left(x_0 - \frac{2x_0}{\pi} \sum_{k=1}^{\infty} \frac{\sin\left(\frac{\pi k x}{x_0}\right)}{k} \right) + x_0. \tag{2}$$

The RFT allows us to approach an ideal step-wise TF very closely when increasing the number of harmonics [see Fig. 1(a)], whereas after keeping the first-order term and notating π/x_0 as β and $2x_0/\pi$ as α, one obtains

$$y_{\text{RFT}} = F(x) = x + \alpha \sin(\beta x). \tag{3}$$

The transfer function is symmetric with respect to zero $F(x) = F(-x)$ and is applied independently to both quadratures, i.e., $y_{R,I} = F(x_{R,I})$, where x_R is the real and x_I the imaginary part of the optical signal. In addition, the α, β parameters define the location and the efficiency of the regenerative areas on the applied transformation. Multiple equidistant plateaus exist at the points $x_{R,I}(k) = (2k+1)\pi/\beta \;\; k \in Z$ for the condition $\alpha\beta = 1$ [see Fig. 1(a)]; however, noise suppression can be achieved also for suboptimal parameters in the range $0 < \alpha\beta < 2$ [8,12].

To realize this transformation, the scheme of Fig. 2 is proposed. It consists of a symmetric Mach–Zehnder interferometer (MZI) with a NOLM and a phase sensitive amplifier (PSA) [13] in each arm to regenerate independently the two signal quadratures. The scheme can be reduced to a single NOLM+PSA configuration by exploiting the polarization dimension.

In each NOLM, the incoming signal is split in counterclockwise and clockwise parts (here and further all the couplers have 1:1 coupling ratio), which are given by

$$E_1 = \frac{i}{2}(x_R + i x_I), \qquad E_1' = \frac{1}{2}(x_R + i x_I). \tag{4}$$

The counterclockwise propagating signal is coupled coherently with a pulsed pump wave of variable duty cycle and peak amplitude ξ, where we assume $\xi \gg x_{R,I}$:

$$E_2 = \frac{1}{\sqrt{2}}\left[\frac{i^2}{2}(x_R + i x_I) + \xi\right], \qquad E_2' = E_1', \tag{5}$$

and, subsequently transmitted via length L of highly nonlinear fiber (HNLF) with zero dispersion, resulting in

$$E_3 = E_2 e^{i\gamma L[|E_2|^2 + 2\langle |E_2'|^2\rangle]}. \tag{6}$$

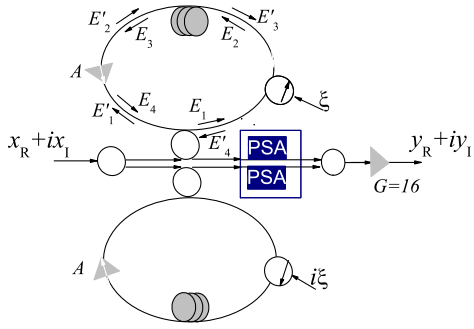

Fig. 2. Scheme: the signal is split in two copies and each one of them is launched to an asymmetric NOLM configuration. At the interferometer, the counterclockwise-propagating signal is mixed with a strong pump wave and undergoes a nonlinear transformation, while the clockwise-propagating signal remains almost unaffected. Afterward, both waves are coupled together and their real part is selected by a PSA element. The regenerated signal quadratures are finally coupled together at the output of the MZI.

We choose the pump to be much stronger than the signal $\xi \gg x_{R,I}$, and we consider the signal-signal interactions to be small (which is usually the case) $\gamma L x_{R,I}^2 \ll 1$; additionally, we compensate the constant nonlinear phase shift $\gamma L \xi^2/4$ (alternatively, one can choose parameters so that $\gamma L \xi^2/4 = 2\pi n$, $n \in Z$), so that

$$E_3 \simeq \frac{\xi}{\sqrt{2}} e^{-i\xi x_R \gamma L/2}. \tag{7}$$

Similarly, for the clockwise-propagating wave we omit $\gamma L x^2 \ll 1$ terms and compensate the constant nonlinear phase shift $\gamma L \xi^2/4$; since $\langle x_{R,I}\rangle = 0$, we derived

$$E_3' = E_2' e^{i\gamma L[|E_2'|^2 + 2\langle |E_2|^2\rangle]} \simeq E_2'. \tag{8}$$

Next, the counterclockwise propagating wave is attenuated by a directional attenuator ([14]) with the attenuation coefficient A; meanwhile, the counter-propagating wave remains unchanged: $E_4' = E_3'$. Coupling E_4 and E_4' and so, we couple two waves and then select the real part, this results in

$$E_R = \mathrm{Re}\left(\frac{E_4' + iE_4}{\sqrt{2}}\right) = \frac{1}{\sqrt{8}}\left(x_R + \sqrt{A}\xi \sin\left(\frac{\xi x_R \gamma L}{2}\right)\right). \tag{9}$$

Similar derivations will hold for the second NOLM element with clockwise and counterclockwise waves interchanged, resulting in the nonlinear transformation of the imaginary signal part.

The transformed quadratures are then coupled together and amplified by gain $G = 16$ to restore the original signal power. This results in the first- order RFT applied independently to both quadratures:

$$y_R + i y_I = \frac{\sqrt{G}}{\sqrt{2}}(E_R + E_I) = F(x_R) + iF(x_I) \tag{10}$$

$$F(x_{R,I}) = x_{R,I} + \alpha \sin(\beta x_{R,I}), \qquad \alpha = \xi\sqrt{A}, \beta = \frac{\xi\gamma L}{2}.$$

For regenerating 4-, 16-, 64-, and 256-QAM signals, nonlinear phase shifts of π, 3π, 7π, and 11π, respectively,

are required; as an example, the TF for regenerating 64-QAM signals is shown in Fig. 1(b). This can be achieved by various combinations of fiber length L and pump power levels. By varying the HNLF length (which affects the value of β), one changes the positioning and number of regenerative levels, whereas by optimizing the attenuation coefficient A (this defines α), we can adjust steepness of the TF and, for $\alpha\beta = 1$, one can obtain plateau levels. The output of the proposed regenerator deviates from the desired first-order RFT for large values of amplitude, when the condition $\xi \gg x$ is not satisfied.

In real fiber-based implementations, stimulated Brillouin scattering (SBS) is expected to be a serious liming factor if we assume operation with a continuous pump wave. This will necessitate the adoption and further improvement of recently proposed SBS suppression methods in the design and fabrication of the nonlinear fiber medium [15]. Alternatively, the SBS effect can be mitigated by operating with short pump pulses, the duration of which should be a fraction of the symbol period and much shorter than the phonon lifetime (~10 ns). In that case, the proposed RFT scheme would be a part of a 3R regenerator that would include additional subsystems for the timing synchronization of the pump pulses to the incoming signal pulses.

Subsequently, we evaluated the proposed RFT by simulating numerically the transmission of rectangular 4-,16-, 64-, and 256-QAM signals through a noisy channel of cascaded regenerators, and compared their performance against the unregenerated case. The signal distortion was modeled as additive white Gaussian noise distributed uniformly along the transmission line, whereas equidistant placement of the regenerators was considered. Our focus was on the noise suppression capabilities of the RFT scheme; therefore, the sections between the regenerators were represented by linear transmission lines, ignoring any other nonlinear or dispersive effect. Timing jitter phenomena also had been neglected, i.e., by assuming a 3R functionality, which allowed us to represent the overall system as a cascade of noise elements, and transfer functions and perform the simulations at one sample per symbol. Thus, for simplicity, the point-to-point transmission system may be characterized by a single parameter, i.e., the signal-to-noise ratio (SNR), defined as the ratio of the average signal power at the input of the transmission system to the total power of the linearly added noise along the line [16]. This is equivalent to the signal-to-noise ratio of the corresponding linear system, i.e., at the absence of regenerative elements, and provides a common reference for a fair comparison of systems with different regenerative properties.

We calculated a symbol error rate (SER) by performing direct error counting on simulated 2^{25} equiprobable symbols as a function of the SNR. As shown in Fig. 3, on the example of a rectangular 16-QAM with 10 equidistantly placed regenerators with different TFs: increasing the number of RFT harmonics leads to better performance; however, even single harmonic enables significant noise suppression. Further, varying the number of first-order RFT regenerators, we evaluated SER for rectangular 16- and 64-QAM signals. The results are depicted in Fig. 4, showing a dramatic improvement of the SER by several orders of magnitude. Note that the achieved regeneration gain scales with the constellation complexity of the signal.

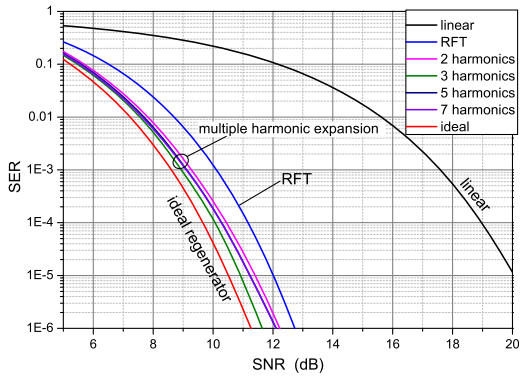

Fig. 3. SER as a function of the SNR for 16-QAM signals for 10 equidistant regenerators with various TF.

Comparing the SER performance when the first-order RFT is used (see Fig. 4, red curves) to that of using an ideal step-wise regenerative transform, we see that the SNR penalty is less than 2 dB. This means that the RFT can enable high regeneration efficiency and improve signal transmission without the need for hard decision based on the use of opto-electronic transponders (Tx/Rx) along the line.

Finally, in Fig. 5, we plotted the constellations of the different QAM signals after transmission via the linear channel (depicted in blue), and compared them to the case where a number of R regenerative elements have been included in the line (depicted in red), with R being equal to 30, 40, and 50. Moving to higher constellation orders, an increased number of cascaded RFT elements and/or SNR had to be considered, since efficient regeneration could be achieved when the SNR$/R$ ratio was less then the size of decision area (i.e., the smallest distance between the neighboring alphabet points) [8]. The suppression of the accumulated noise on both signal quadratures was evident. Furthermore, the RFT-induced squeezing affected the statistics of the residual noise, i.e., the circular symmetry of the initial

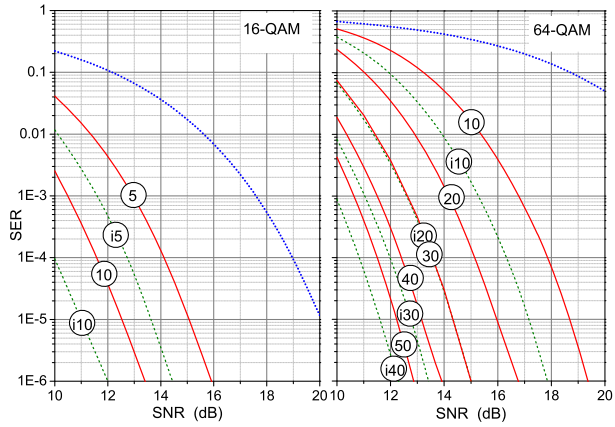

Fig. 4. In red solid lines, the SER as a function of the SNR, for 16- and 64-QAM signals, and for different numbers (in the circle) of cascaded first-order RFT regenerators. The green dashed lines indicate the SER when a number (denoted also by i) of ideal regenerators is considered. Finally, in blue dotted lines, the SER of corresponding linear channels is shown for reference.

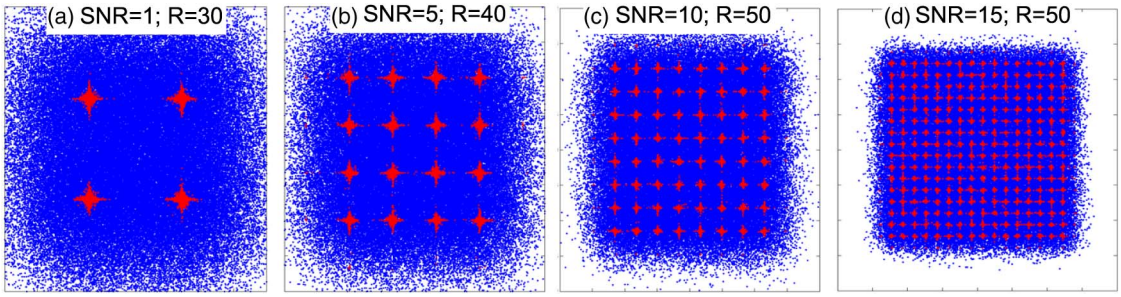

Fig. 5. Constellation diagrams (normalized to average signal power) of rectangular (a) 4-, (b) 16-, (c) 64-, and (d) 256-QAMs signals after propagation through a transmission line with (red) or without (blue) R equidistantly placed first-order RFT regenerators. The depicted SNR (dB) value characterizes the SNR ratio of the corresponding linear system.

Gaussian distribution (blue points) broke into a new axial symmetry (red points). Figure 5 also demonstrated the scalability of the proposed scheme. By tuning only the pump power, the transfer function of the regenerator could be adjusted to handle the different sizes of constellation.

In summary, we proposed a new all-optical regeneration approach for conventional multilevel rectangular QAM formats based on the use of two asymmetric NOLMs +PSA elements in MZI configuration. The scheme realizes a RFT transformation independently on the two signal quadratures enabling efficient suppression of noise distortion. Numerical simulations illustrated a successful cascadability performance for the case of 4-, 16-, 64-, and 256-QAM signals.

Funding. Engineering and Physical Sciences Research Council (EPSRC) (EP/J017582/1, EP/L000091/1); EU-ICT (318415); Marie Currie project (IEF-330697); Royal Society (WM120035).

REFERENCES

1. R. J. Essiambre, G. Kramer, P. J. Winzer, G. J. Foschini, and B. Goebel, J. Lightwave Technol. **28**, 662 (2010).
2. J. Kakande, R. Slavik, F. Parmigiani, A. Bogris, D. Syvridis, L. Gruner-Nielsen, R. Phelan, P. Petropoulos, and D. J. Richardson, Nat. Photonics **5**, 748 (2011).
3. N. J. Doran and D. Wood, Opt. Lett. **13**, 56 (1988).
4. T. Rothlingshfer, G. Onishchukov, B. Schmauss, and G. Leuchs, IEEE Photon. Technol. Lett. **26**, 556 (2014).
5. T. Roethlingshoefer, T. Richter, B. Stiller, G. Onishchukov, C. Schubert, B. Schmauss, and G. Leuchs, Proc. SPIE **8964**, 89640L (2014).
6. M. A. Sorokina, Opt. Lett. **39**, 2499 (2014).
7. T. I. Lakoba and M. Vasilyev, Opt. Express **15**, 10061 (2007).
8. T. I. Lakoba, J. R. Williams, and M. Vasilyev, Opt. Express **19**, 23017 (2011).
9. M. A. Sorokina and S. K. Turitsyn, Nat. Commun. **5**, 3861 (2014).
10. K. Croussore, C. Kim, and G. Li, Opt. Lett. **29**, 2357 (2004).
11. M. Marhic and C. Hsia, Quantum Opt. **3**, 341 (1991).
12. M. A. Sorokina, S. Sygletos, and S. K. Turitsyn, Opt. Lett. **38**, 4378 (2013).
13. C. J. McKinstrie and S. Radic, Opt. Express **12**, 4973 (2004).
14. A. Striegler, M. Meissner, K. Cvecek, K. Sponsel, G. Leuchs, and B. Schmauss, IEEE Photon. Technol. Lett. **17**, 639 (2005).
15. L. Grner-Nielsen, D. Jakobsen, S. Herstrm, B. Plsdttir, S. Dasgupta, D. Richardson, C. Lundstrm, S. Olsson, and P. Andrekson, "Brillouin suppressed highly nonlinear fibers," in *European Conference in Optical Communications* (Optical Society of America, 2012), paper We.1.F.1.
16. M. Sorokina, S. Sygletos, A. D. Ellis, and S. K. Turitsyn, Opt. Express **21**, 31201 (2013).